ISSN: 2717-8161 RESEARCH ARTICLE

New Trends in Medicine Sciences

New Trend Med Sci 2020; 1(1): 6-13 https://dergipark.org.tr/tr/pub/ntms

Diffusion Tensor Imaging of Metastatic Axillary Lymph Nodes

Irmak Durur-Subasi[1,2,3*], Fatih Alper[3], Pınar Tuncel-Eyi[2], Adem Karaman[3], Veysel Esdur[3], Elif Demirci[4], Baki Hekimoğlu[2]

[1] Department of Radiology, Faculty of Medicine, İstanbul Medipol University, Istanbul, Turkey
[2] Clinic of Radiology, Diskapi Yildirim Beyazit Training and Research Hospital, University of Health Sciences, Ankara, Turkey
[3] Department of Radiology, Faculty of Medicine, Atatürk University Erzurum, Turkey
[4] Department of Pathology, Faculty of Medicine, Atatürk University, Erzurum, Turkey

Article History
Received 24 May 2020
Accepted 03 June 2020
Published Online 15 June 2020

[*]***Corresponding Author***
Irmak Durur-Subasi MD, PhD,
Istanbul Medipol University
Faculty of Medicine
Department of Radiology
Istanbul, Turkey
E-mail: irmakdurur@yahoo.com
Phone: +905334603846
Fax: +902124607070
ORCID: http://orcid.org/0000-0003-3122-4499

Abstract: It was aimed to investigate whether the fractional anisotropy (FA) differs for the benign and metastatic axillary lymph nodes (LNs). 58 women with benign (n=33) and metastatic (n=25) axillary LNs who underwent diffusion-weighted and tensor imaging with a 3T scanner were enrolled. Apparent diffusion coefficient (ADC) and FA, cortex thickness, long and short axes were measured retrospectively and compared statistically. Observer reliabilities were also assessed in terms of intra and inter-reviewer variability. Metastatic LNs showed significantly lower ADC and FA values and greater cortex thickness, long and short axes. ROC test showed the area under the curve values of 0.876 for ADC, 0.661 for FA, and 0.960 for cortex thickness. Cortex thickness had excellent sensitivity, specificity, and accuracy. A cutoff value of 3.5 mm for cortex thickness had 92% sensitivity, 94% specificity, 92% positive predictive value (PV), 93% negative PV, and 93% accuracy. A cutoff value of 0.774×10^{-3} mm^2/s for ADC had 84% sensitivity, 82% specificity, 79% positive PV, 90% negative PV, and 84% accuracy. A cutoff value of 0.423×10^{-3} mm^2/s for FA had 64% sensitivity, 76% specificity, 67% positive PV, 71% negative PV, and 71% accuracy. High intra- and inter-observer reliabilities were seen. Among the parameters assessed by our study, cortex thickness had superior accuracy. ADC and FA showed a respectable diagnostic performance, especially the first one having a high negative PV and the second one relatively high specificity. © 2020 NTMS.

Keywords: Axilla, Apparent Diffusion Coefficient, Diffusion Tensor Imaging, Fractional Anisotropy, Lymph Nodes, Magnetic Resonance Imaging.

1. Introduction

Diagnosing axillary lymph node (LN) involvement is important in breast carcinoma management because LN status changes treatment decisions (1,2). Although sentinel biopsy is generally done in invasive breast cancer, axilla dissection continues to be performed in patients with invasive, high-grade carcinomas (1,3).

Magnetic resonance imaging (MRI) with its superior latitudinal resolution and tissue categorization capacity has the uppermost sensitivity for the discovery of breast carcinoma (4,5).

On the other hand, its moderate specificity leads to the search for additional supportive tools.

Cite this article as: Durur-Subasi I, Alper F, Tuncer P, Karaman A, Esdur V, Demirci E, Hekimoğlu B. Diffusion tensor imaging of metastatic axillary lymph nodes. *New Trend Med Sci* **2020**;1 (1): 6-13.

Diffusion tensor and diffusion-weighted imaging (DTI and DWI) are two advanced MRI tools and are currently active research areas with this point of view (6-10).
Although many studies have been conducted on breast DWI, few studies have reported on DTI for breast and no DTI study for axilla (11-16). DTI applies extra gradients to identify the amount of diffusion and allows the evaluation of the extent of anisotropic diffusion in concerned tissue, referred to as the full diffusion tensor (11). Fractional anisotropy (FA) deals with the amount of anisotropy, while the apparent diffusion coefficient (ADC) is the directionally averaged diffusivity (17).
According to our knowledge, DTI has not been previously used to evaluate axillary LNs.
In this study, we studied the importance of the FA parameter for benign and metastatic axillary LNs.

2. Patients and Methods

The institutional ethics committee of our university hospital appropriated the retrospectively designed procedure, and informed-consent was surrendered (2301-13/1).

2.1. Patients

We reviewed our archives and identified 58 women with benign (n=33) and metastatic (n=25) axillary LNs between July 2013 and October 2015. Axillary LNs of patients with Breast Imaging-Reporting and Data System (BI-RADS) category 1-2 results on MRI, no suspicious findings on conventional imaging, no change in findings over 2 years, and histopathological evidence of benign breast pathology were involved in the benign group. Patients with breast carcinoma and pathologically proven ipsilateral metastatic LNs were included in the metastatic group. When several nodes were detected, the biggest one was measured.
Exclusion criteria were previous chemotherapy for breast carcinoma, incomplete examination, or un-diagnosable images (e.g. due to artifacts or distortions, or lack of coil cover).

2.2. Breast MRI

Breast MRI was acquired by a 3-Tesla scanner (Skyra; Siemens, Germany) and a dedicated coil with patients in the prone position. A standard protocol was used: coronal short time inversion recovery (STIR), sagittal fat-suppressed, turbo-spin echo T2-weighted imaging, turbo-spin echo T1-weighted imaging, single-shot echo-planar imaging (as DWI) and dynamic pre- and post-contrast fat-suppressed, fast low-angle shot (FLASH) three-dimensional images were acquired.

2.3. DWI and DTI

DWI and DTI were acquired with the following parameters: TR=4000-ms, TE=60-ms, slice thickness=4.0-mm, FOV=380-mm, averages=4, interslice gap=0 and scan time=3.37-min. Diffusion gradients were applied in 6 directions with b=50, 400, and 800 s/mm^2 in all cases.

2.4. Interpretations

Breast MRI, DWI, and DTI data were post-processed on the MRI console using the Neuro3D toolbox (Leonardo, Siemens Healthcare, Erlangen, Germany). The cortex thickness, greatest long and short axes of the LNs was measured on the post-contrast T1-weighted image. The DWI and DTI parameters were calculated by tracing a free-hand region of interest (ROI) on the cortex of the LNs on ADC and FA map by a simultaneous display with T1-WI. The two-dimensional ROI was cautiously positioned on the LN to include the cortex and exclude the necrotic and cystic components, axillary fat, or hilum. The ROI size was variable depending on the anatomy and size of the LN. ROI calculations were done by a radiologist with 15-year-experienced (AK) who was blinded to the patients' history and histological results at least three times. Intraobserver consistency was evaluated by the same radiologist at a time interval of two weeks, and the same information was used with a second radiologist with 5 years of experience (VE) to assess inter-observer reliability.

2.5. Statistics

The statistics were done by IBM SPSS Statistics for Windows, Version 21.0. Distribution normality was determined by the Shapiro-Wilk test. The cortex thickness, long and short axes, ADCs, and FAs were compared by independent samples *t*-test between the benign and metastatic lesions. Receiver operating characteristic (ROC) curve analysis was performed to define the cutoff points and diagnostic performances. Intraobserver agreement was calculated by the Pearson correlation coefficient and interobserver agreement by Kendall's coefficient of concordance (the mean value of the first observer compared with the second observer's measurement). All tests were two-tailed and a p-value under 0.05 was accepted as a statistical significance level.

3. Results

A total of 33 female (mean age=41±7 (32-50) years) were enrolled in the benign group and 25 female patients (mean age=50±13 (26-80) years) with pathologically proven metastatic axillary involvement comprised the metastatic group (Figures 1, 2).
For the benign group, the mean long axis was 16±5-mm (between 9-31-mm) and the mean short axis was 9±3-mm (between 5-17-mm). For the metastatic group, the mean long axis was 26±21-mm (between 10-95-mm) and the mean short axis was 22±17-mm (between 8-78-mm).
Statistical analyses showed significant changes in ADC (P=0.00), and FA values (P=0.04) cortex thickness (P<0.00), long (P=0.00) and short axes (P=0.00), (Table 1). The metastatic group had a significantly greater size and cortex thickness, lower ADC and FA values (Figures 3, 4).
ROC analysis showed the area under the curve value of 0.876 for ADC and 0.661 for FA values, 0.960 for

cortex thickness, 0.687 for long axis, 0.848 for short axis (Figures 5, 6; Table 2). A cutoff value of 3.5 mm for cortex thickness had 92% sensitivity, 94% specificity, 92% positive predictive value (PV), 93% negative PV and 93% accuracy. A cutoff value of $0.774x10^{-3}$ mm^2/s for ADC had 84% sensitivity, 82% specificity, 79% positive PV, 90% negative PV and 84% accuracy. A cutoff value of 0.423 $x10^{-3}$ mm^2/s for FA had 64% sensitivity, 76% specificity, 67% positive PV, 71% negative and 71% accuracy (Figure 7).

High intra- and inter-observer agreements were seen for ADC (R=0.917, P=0.00 and R=0.761, P=0.00) and FA values (R=0.876, P=0.00 and R=0.700, P=0.00), cortex thickness (R=0.910, P=0.00 and R=0.850, P=0.00), for long axis (R=0.956, P=0.00 and R=0.887, P=0.00), short axis (R=0.970, P=0.00 and R=0.910, P=0.00).

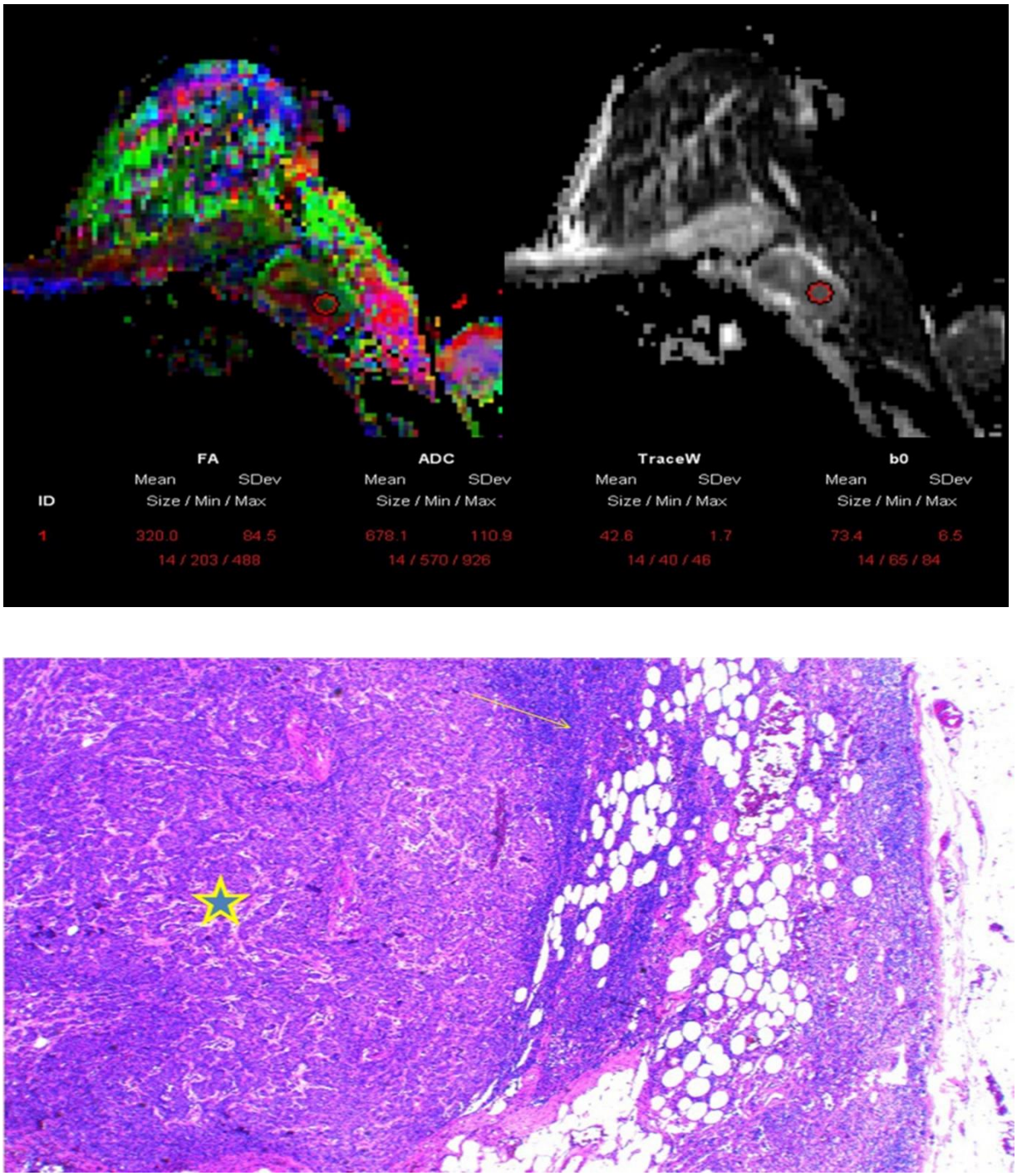

Figure 1: A case of metastatic axillary involvement on the left. Thickened cortex, round configuration and hilar obliteration can be seen (a). Pathology specimen shows lymphoid tissue (arrow) and metastasis (star) (b).

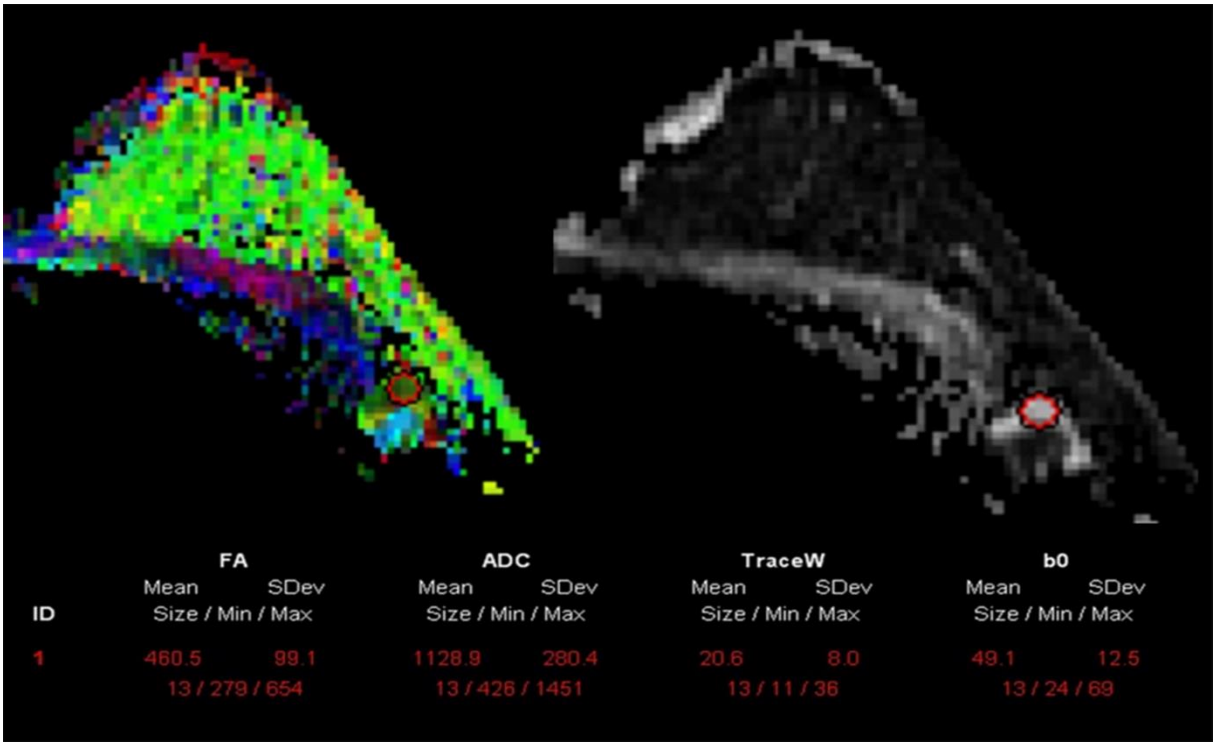

Figure 2: A benign lymph node with a thin cortex is visible in the left axilla.

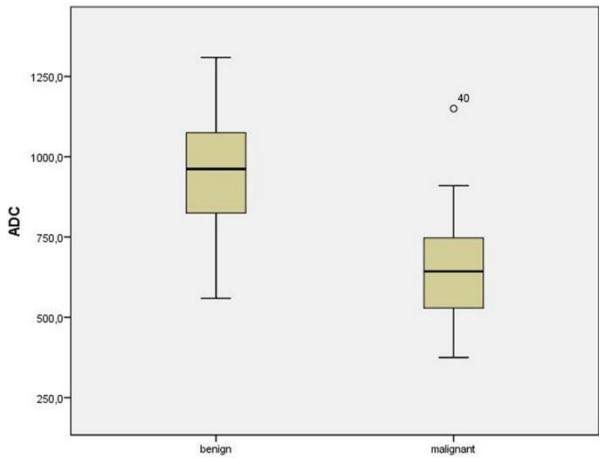

Figure 3: Box plot shows ADC values of benign and metastatic lymph nodes. Boxes symbolize interquartile range divided at the median; whiskers show range of all values. Circles and diamonds represent outliers. Metastatic nodes show lower ADC values.

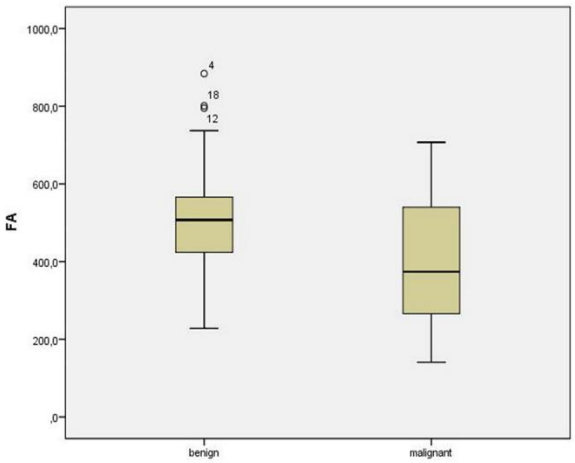

Figure 4: Box plot shows FA values of benign and metastatic lymph nodes. Boxes symbolize interquartile range divided at the median; whiskers show range of all values. Circles and diamonds represent outliers. Metastatic nodes show lower FA values.

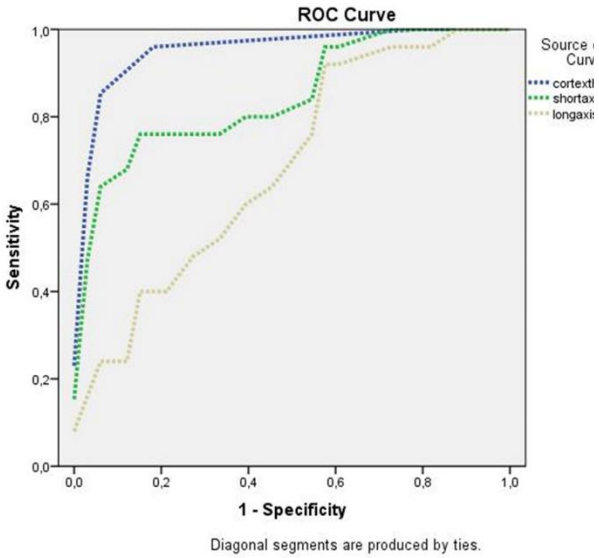

Figure 5: In receiver operating characteristic (ROC) curve analysis, cortex thickness has the highest area under the curve (AUC) value.

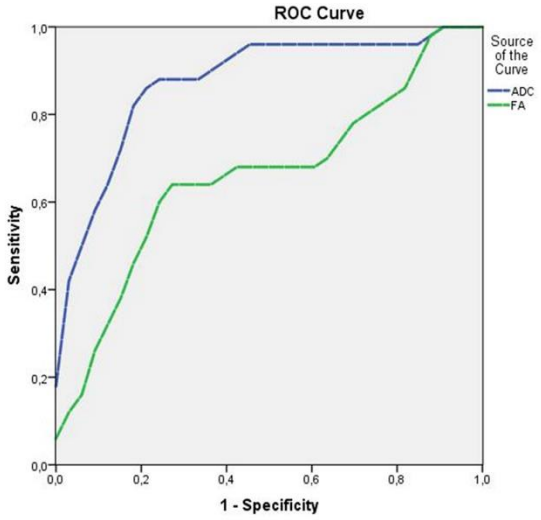

Figure 6: Receiver operating characteristic (ROC) curve analysis shows a high area under the curve (AUC) value of ADC.

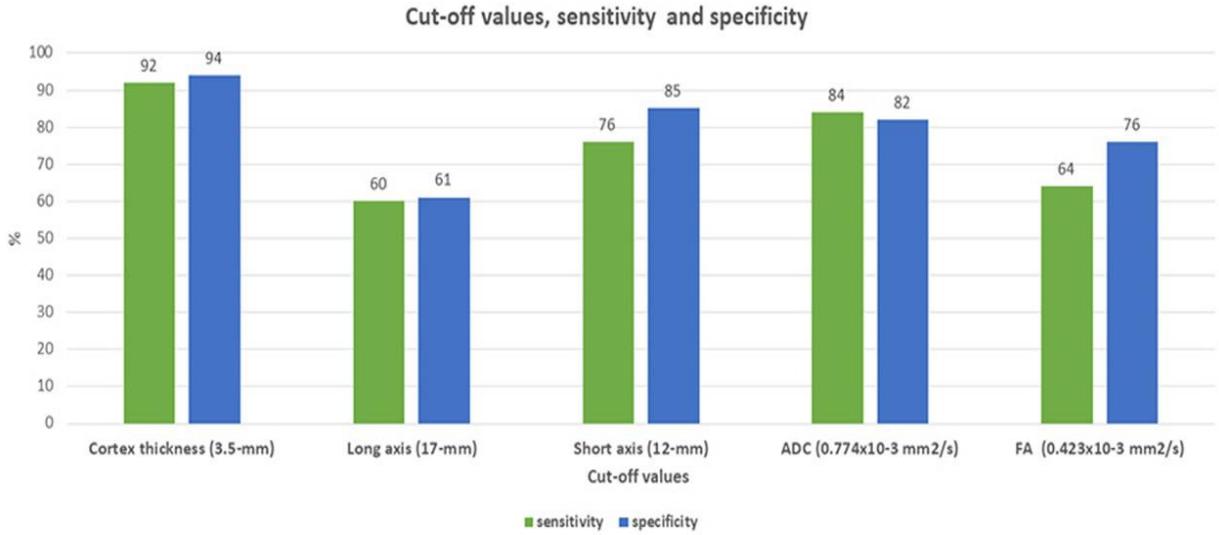

Figure 7: Graphic shows cutoff values obtained by ROC analysis and sensitivity and specificity combinations.

4. Discussion

In this study, we evaluated ADC and FA values, cortex thickness, short-long axes of benign and metastatic axillary LNs. Metastatic LNs showed significantly greater cortex thickness and short-long axes, lower ADC and FA values. Cortex thickness had an excellent diagnostic performance. ADC value had a relatively good diagnostic performance with especially a high negative PV of 90%. FA had a moderate diagnostic performance with remarkable specificity.

Staging axilla by LN dissection is highly accurate. However, due to morbidities such as lymphedema and paresthesia following this procedure, the development of non-invasive, image-based methods for detecting axillary LN metastasis is an active research area. There is no characteristic finding on dynamic MRI with high specificity for the distinction between benign and metastatic LNs (18).

Although several studies have suggested that DWI has some utility in axillary LN assessment (19), there is a paucity of data in the English literature concerning DTI parameters of axillary LNs.

ADC values obtained by DWI were reported as useful in discriminating benign and metastatic LNs by some authors, but not others (20-22). Rautiainen et al. imaged 56 axillae (121 LNs) and concluded that metastatic axillary LNs consumed significantly lower ADC values ($P<0.001$). According to their results, mean ADC as obtained by 3-T was $0.663\text{-}0.676 \times 10^{-3}$ mm^2/s for metastatic LNs and $1.100\text{-}1.225 \times 10^{-3}$ mm^2/s for benign ones (maximum *b* value of 800 s/mm^2) (21).

Yamaguchi et al. evaluated pathologically proven axillary LNs with and without metastasis and determined a mean ADC value of 0.746×10^{-3} mm^2/s for metastatic LNs and 1.033×10^{-3} mm^2/s for non-metastatic LNs (maximum *b* value of 800 s/mm^2) ($P<0.001$). They reported 85% sensitivity and 81% specificity by a cutoff ADC value of $0.852x10^{-3}$ mm^2/s to differentiate metastatic from non-metastatic LNs (23).

In contrast, Kamitani et al. studied axillary LNs with and without metastasis on a 1.5-T system and concluded that the ADC of metastatic nodes was considerably higher than that of benign LNs (1.08×10^{-3} mm^2/s vs. 0.92×10^{-3} mm^2/s, maximum *b* value of 1000 s/mm^2, $P=0.004$) (24). According to our results, benign LNs had higher mean ADC values than metastatic ones (0.965×10^{-3} mm^2/s vs. 0.669×10^{-3} mm^2/s) and the difference was statistically significant (maximum *b* value of 800 s/mm^2).

Additionally, ROC analysis showed that an ADC cutoff of $0.774x10^{-3}$ mm^2/s had high sensitivity and specificity. Especially negative PV was better.

DWI is reported to provide information about tissue microenvironments such as perfusion, flow effects, cell density, proliferation rate, nucleus size, intracellular macromolecules, nucleus/cytoplasm ratio and extracellular matrix volume (25-31). ADC values are considered to represent the cellular or extracellular elements of the tissue, while FA values are believed to reflect tissue organization (14). The lower FA values reported representing more organized tissues.

Table 1: Differences of size, diffusion tensor imaging (DTI) and diffusion-weighted imaging (DWI) parameters of axillary lymph nodes.

Variable(s)	Group	N	Mean	Standard Deviation	P values
Cortex thickness (mm)	Benign	33	2.2	1.3	0.00*
	Metastatic	25	10.8	9.1	
Long axis (mm)	Benign	33	16	5	0.00*
	Metastatic	25	26	21	
Short axis (mm)	Benign	33	9	3	0.00*
	Metastatic	25	22	17	
ADC value ($x10^{-3}$ mm^2/s)	Benign	33	0.965	0.186	0.00*
	Metastatic	25	0.669	0.183	
FA value ($x10^{-3}$ mm^2/s)	Benign	33	0.481	0.153	0.04*
	Metastatic	25	0.394	0.151	

Table 2: ROC analysis results, performance of benign-metastatic discrimination of variables.

Variable(s)	Area under curve	95% Confidence Interval	
		Lower Bound	Upper Bound
Cortex thickness	0.960	0.910	1,000
Long axis	0.687	0.551	0.822
Short axis	0.848	0.745	0.951
ADC	0.876	0.783	0.970
FA	0.661	0.514	0.808

DTI studies of breast imaging are limited in number. Partridge et al. reported in their study that anisotropy was reduced in metastatic tumors than the normal parenchyma, but FA did not allow significant discrimination (13). In another study, it is reported that the breast parenchyma showed mainly anterior-posterior diffusion, whereas breast lesions had no principal diffusion direction (14). The metastatic tumors displayed a lower ADC and higher FA and ADC was more distinctive. Cakir et al. studied ADC and FA in 30 malignant and 25 benign lesions as well as normal breast parenchyma. They reported that FA was not discriminative for benign and malignant lesions (11). Tagliafico et al. measured ADC and FA values of normal breast tissue at 3.0 T and concluded that ADC values obtained with DTI are more reproducible than FA (15). Jiang et al. studied DTI of breast lesions and concluded ADC and FA values are statistically different between benign and malignant lesions and associated with cellularity. To their results, ADC was useful to estimate the grade (32). Our study showed a better diagnostic performance of ADC than FA, and the

first one was considerably different for benign and metastatic LNs much more. So ADC was more reproducible than FA.

A limitation of the present study is its retrospective design. Secondly, there may be potential population bias because the axilla was not fully covered by the coil during DWI/DTI for every patient examined in our department. The number of patients was also limited. For the benign group, diagnostic confirmation was based on clinical, radiologic and follow-up data but there was no histopathological analysis and some benign LNs too small for ROI placement were not evaluated. In the metastatic group, histopathological results were available, but no marking procedure had been performed. Additionally, no normalization was used for parameters.

5. Conclusions

In conclusion, to our understanding, this is the first study using DTI to evaluate axillary LNs. Metastatic LNs presented significantly greater cortex thickness and short-long axes, lower ADC and FA values. ADC value had a relatively better diagnostic performance than FA.

Institutional review board (IRB) statement

IRB approved the study.

Informed consent statement

No informed consent due to retrospective design.

Conflict of interest statement

No conflict of interests.

Funding statement

No funding received.

References

1. Fornasa F, Nesoti MV, Bovo C, et al. Diffusion-weighted magnetic resonance imaging in the characterization of axillary lymph nodes in patients with breast cancer. *J Magn Reson Imaging* **2012**; 36: 858-864.
2. Silverstein MJ, Skinner KA, Lomis TJ. Predicting axillary nodal positivity in 2282 patients with breast carcinoma. *World J Surg* **2001**; 25:767–772.
3. Mansel RE, Fallowfield L, Kissin M etal. Randomized multicenter trial of sentinel node biopsy versus standard axillary treatment in operable breast cancer: the ALMANAC trial. *J Natl Cancer Inst* **2006**; 98:599–609.
4. Durur-Subasi I, Durur-Karakaya A, Alper F etal. Breast lesions with high signal intensity on T1-weighted MR images. *Jpn J Radiol* **2013**; 31: 653-661.
5. Durur-Subasi I, Alper F, Akcay MN, et al. Magnetic resonance imaging findings of breast juvenile papillomatosis. *Jpn J Radiol* **2013**; 31: 419-423.
6. Durur-Subasi I, Durur-Karakaya A, Karaman A, et al. Is the necrosis/wall ADC ratio useful for the differentiation of benign and malignant breast lesions? *Br J Radiol* **2017**; 90: 20160803.
7. Durur-Subasi I, Durur-Karakaya A, Karaman A et al. Value of MRI sequences for prediction of invasive breast carcinoma size. *J Med Imaging Radiat Oncol* **2014**; 58: 565-568.
8. Durur-Karakaya A, Seker M, Durur-Subasi I. Diffusion-Weighted Imaging in Ectopic Pregnancy: Ring of Restriction Sign. *Br J Radiol* **2017**; 90: 20170528.
9. Pinker K, Helbich TH, Morris EA. The potential of multiparametric MRI of the breast. *Br J Radiol* **2017**; 90: 20160715.
10. Guvenc I, Akay S, Ince S et al. Apparent diffusion coefficient value in invasive ductal carcinoma at 3.0 Tesla: is it correlated with prognostic factors? *Br J Radiol* **2016**; 89: 20150614.
11. Cakir O, Arslan A, Inan N et al. Comparison of the diagnostic performances of diffusion parameters in diffusion weighted imaging and diffusion tensor imaging of breast lesions. *Eur J Radiol* **2013**; 82: 801–806.
12. Eyal E, Shapiro-Feinberg M, Furman-Haran E et al. Parametric diffusion tensor imaging of the breast. *Invest Radiol* **2012**; 47: 284-291.
13. Partridge SC, Ziadloo A, Murthy R et al. Diffusion tensor MRI: preliminary anisotropy measures and mapping of breast tumors. *J Magn Reson Imaging* **2010**; 31: 339-347.
14. Baltzer PA, Schäfer A, Dietzel M et al. Diffusion tensor magnetic resonance imaging of the breast: a pilot study. *Eur Radiol* **2011**; 21: 1-10.
15. Tagliafico A, Rescinito G, Monetti F etal. Diffusion tensor magnetic resonance imaging of the normal breast: reproducibility of DTI-derived fractional anisotropy and apparent diffusion coefficient at 3.0 T. *Radiol Med* **2012**; 117: 992-1003.
16. Kim JY, Kim JJ, Kim S, Choo KS, Kim A, Kang T, Park H. Diffusion tensor magnetic resonance imaging of breast cancer: associations between diffusion metrics and histological prognostic factors. *Eur Radiol* **2018**; 28: 3185-3193.
17. Jaimes C, Darge K, Khrichenko D, et al. Diffusion tensor imaging and tractography of the kidney in children: feasibility and preliminary experience. *Pediatr Radiol* **2014**; 44: 30-41.
18. Partridge SC, Nissan N, Rahbar H, et al. Diffusion-weighted breast MRI: Clinical applications and emerging techniques. *J Magn Reson Imaging* **2017**; 45: 337-355.
19. Kim SH, Shin HJ, Shin KC et al. Diagnostic Performance of Fused Diffusion-Weighted Imaging Using T1-Weighted Imaging for Axillary Nodal Staging in Patients With Early Breast Cancer. *Clin Breast Cancer* **2017**; 17:154–63.
20. Xing H, Song CL, Li WJ. Meta analysis of lymph node metastasis of breast cancer patients: clinical value of DWI and ADC value. *Eur J Radiol* **2016**; 85: 1132-1137.
21. Rautiainen S, Könönen M, Sironen R et al. Preoperative axillary staging with 3.0-T breast MRI: clinical value of diffusion imaging and

apparent diffusion coefficient. *PLoS One* **2015**; 10: 0122516.
22. Rahbar H, Conlin JL, Parsian S, et al. Suspicious axillary lymph nodes identified on clinical breast MRI in patients newly diagnosed with breast cancer: can quantitative features improve discrimination of malignant from benign? *Acad Radiol* **2015**; 22: 430-438.
23. Yamaguchi K, Schacht D, Nakazono T, et al. Diffusion weighted images of metastatic as compared with nonmetastatic axillary lymph nodes in patients with newly diagnosed breast cancer. *J Magn Reson Imaging* **2015**; 42: 771-778.
24. Kamitani T, Hatakenaka M, Yabuuchi H et al. Detection of axillary node metastasis using diffusion-weighted MRI in breast cancer. *Clin Imaging* **2013**; 37: 56-61.
25. Karaman A, Durur-Subasi I, Alper F, et al. Is it better to include necrosis in apparent diffusion coefficient (ADC) measurements? The necrosis/wall ADC ratio to differentiate malignant and benign necrotic lung lesions: Preliminary results. *J Magn Reson Imaging* **2017**; 46:1001-1006.
26. Iannicelli E, Di Pietropaolo M, Pilozzi E et al. Value of diffusion-weighted MRI and apparent diffusion coefficient measurements for predicting the response of locally advanced rectal cancer to neoadjuvant chemoradiotherapy. *Abdom Radiol (NY)* **2016**; 41: 1906-1917.
27. Nesbakken A, Nygaard K, Westerheim O, et al, Local recurrence after mesorectal excision for rectal cancer. *Eur J Surg Oncol* **2002**; 28: 126-134.
28. Kapiteijn E, Marijnen CA, Nagtegaal ID et al. Preoperative radiotherapy combined with total mesorectal excision for resectable rectal cancer. *N Engl J Med* **2001**; 345: 638-646.
29. Henzler T, Schmid-Bindert G, Schoenberg SO, et al. Diffusion and perfusion MRI of the lung and mediastinum. *Eur J Radiol* **2010**; 76: 329-336.
30. Durur-Subasi I. DW-MRI of the breast: a pictorial review. *Insights Imaging*. **2019**; 10(1): 61.
31. Durur-Subasi I. Diagnostic and Interventional Radiology in Idiopathic Granulomatous Mastitis. *Eurasian J Med*. **2019**; 51(3): 293-297.
32. Jiang R, Ma Z, Dong H, et al. Diffusion tensor imaging of breast lesions: evaluation of apparent diffusion coefficient and fractional anisotropy and tissue cellularity. *Br J Radiol* **2016**; 89: 20160076.

Authors' ORCID
Irmak Durur Subasi
http://orcid.org/ 0000-0003-3122-4499
Fatih Alper
http://orcid.org/0000-0002-9483-8861
Pınar Tuncel-Eyi
http://orcid.org/0000-0002-2417-8546
Adem Karaman
http://orcid.org/0000-0002-3091-0609
Veysel Esdur
http://orcid.org/0000-0001-6729-3600
Elif Demirci
http://orcid.org/0000-0002-6660-3870
Baki Hekimoğlu
http://orcid.org/0000-0002-1824-5853

https://dergipark.org.tr/tr/pub/ntms